J|A|C|S
ARTICLES
Published on Web 10/30/2007

Nanostructured Silica Thin Films Self-Assembled with Electron Donors and Acceptors to Measure Electron Tunneling

Erik Johansson and Jeffrey I. Zink*

Contribution from the Department of Chemistry and Biochemistry, University of California, Los Angeles, California 90095

Received July 17, 2007; E-mail: zink@chem.ucla.edu

Abstract: Surfactant-templated, mesostructured thin films are synthesized such that photoelectron donors and electron acceptors are separated spatially in the different regions of the thin film. A photoelectron donor is placed within the silica framework by using a silylated derivative of the well-known tris(bipyridine)-ruthenium(II) cation. Selective placement of the electron acceptor is achieved by using a surfactant derivative of methyl viologen. Luminescence decay traces and luminescence spectra are collected for the electron donor in the presence of varying amounts of the electron acceptor. Because of the spatial separation of the donor and acceptor noncontact electron transfer occurs and the electron-transfer rate decreases exponentially with the distance separating the donor and acceptor. Luminescence decay traces are calculated and fit to the experimental data in order to extract a value for the contact quenching rate, k_0 (s^{-1}), as well as the exponential decay constant β ($Å^{-1}$) which governs how fast the electron-transfer rate decreases as a function of the donor−acceptor distance. The value $\beta = 2.5 \pm 0.4$ $Å^{-1}$ shows that the mesostructured material is an excellent insulator, better than frozen organic glasses or proteins and approaching that of vacuum. Combining deliberate placement methods, spectroscopy, and calculations has made possible the first measurement of β for the silica region of mesoporous thin films.

Introduction

Inorganic oxide materials and their synthesis by the sol−gel method are extensively reviewed topics.[1−3] Out of the many oxide materials that can be synthesized by sol−gel methods, silica has drawn the most attention. The sol−gel method employs relatively gentle conditions for making oxide materials and is thus well suited for incorporating molecules into the materials synthesized. Early functional sol−gel materials were made by physically immobilizing molecules and biomolecules such as enzymes in the sol−gel matrix, and this area remains under active investigation.[4−11]

In 1992 the first example of mesostructured silica in the form of surfactant-templated particles was reported.[12] Since then, both mesostructured particles, and more recently films,[13−17] have been well studied, and an extensive background has developed on the self-assembly of metal oxides based on surfactant and block copolymers as the structure-directing agents.[3,18−21] In this paper we use a one-step, one-pot method based on evaporation induced self-assembly (EISA) to synthesize mesostructured thin films.[13] This method of synthesizing films consists of dip coating a thin liquid film onto a silicon substrate by immersing the substrate into a sol and withdrawing it at constant speed. The formation of the mesostructured film is driven by the preferential evaporation of ethanol that, by leading to an increase in water, surfactant, and acid concentrations, directs the two-dimensional (2D)-hexagonal liquid crystal formation as well as increases the silica condensation rate (Figure 1). This approach was chosen because

(1) Brinker, C. J.; Scherer, G. W. *Sol-Gel Science: the physics and chemistry of sol-gel processing*; Academic Press Inc.: San Diego, CA, 1990.
(2) Loy, D. A.; Shea, K. J. *Chem. Rev.* **1995**, *95*, 1431.
(3) Soler-Illia, G. J. de A. A.; Sanchez, C.; Lebeau, B.; Patarin, J. *Chem. Rev.* **2002**, *102*, 4093.
(4) Ellerby, L. M.; Nishida, C. R.; Nishida, F.; Yamanaka, S. A.; Dunn, B.; Valentine, J. S.; Zink, J. I. *Science* **1992**, *255*, 1113.
(5) Dave, B. C.; Dunn, B.; Valentine, J. S.; Zink, J. I. *Anal. Chem.* **1994**, *66*, A1120.
(6) Miller, J. M.; Dunn, B.; Valentine, J. S.; Zink, J. I. *J. Non-Cryst. Solids* **1996**, *202*, 279.
(7) Dunn, B.; Miller, J. M.; Dave, B. C.; Valentine, J. S.; Zink, J. I. *Acta Mater.* **1998**, *46*, 737.
(8) Avnir, D.; Braun, S.; Lev, O.; Ottolenghi, M. *Chem. Mater.* **1994**, *6*, 1605.
(9) Avnir, D. *Acc. Chem. Res.* **1995**, *28*, 328.
(10) Chia, S. Y.; Urano, J.; Tamanoi, F.; Dunn, B.; Zink, J. I. *J. Am. Chem. Soc.* **2000**, *122*, 6488.
(11) Dave, B. C.; Miller, J. M.; Dunn, B.; Valentine, J. S.; Zink, J. I. *J. Sol-Gel Sci. Technol.* **1997**, *8*, 629.
(12) Kresge, C. T.; Leonowicz, M. E.; Roth, W. J.; Vartuli, J. C.; Beck, J. S. *Nature* **1992**, *359*, 710.
(13) Lu, Y. F.; Ganguli, R.; Drewien, C. A.; Anderson, M. T.; Brinker, C. J.; Gong, W. L.; Guo, Y. X.; Soyez, H.; Dunn, B.; Huang, M. H.; Zink, J. I. *Nature* **1997**, *389*, 364.
(14) Zhao, D.; Yang, P.; Melosh, N.; Feng, J.; Chmelka, B. F.; Stucky, G. D. *Adv. Mater.* **1998**, *10*, 1380.
(15) Alberius, P. C. A.; Frindell, K. L.; Hayward, R. C.; Kramer, E. J.; Stucky, G. D.; Chmelka, B. F. *Chem. Mater.* **2002**, *14*, 3284.
(16) Huang, M. H.; Dunn, B. S.; Zink, J. I. *J. Am. Chem. Soc.* **2000**, *122*, 3739.
(17) Huang, M. H.; Dunn, B. S.; Soyez, H.; Zink, J. I. *Langmuir* **1998**, *14*, 7331.
(18) Huo, Q. S.; Margolese, D. I.; Ciesla, U.; Demuth, D. G.; Feng, P. Y.; Gier, T. E.; Sieger, P.; Firouzi, A.; Chmelka, B. F.; Schuth, F.; Stucky, G. D. *Chem. Mater.* **1994**, *6*, 1176.
(19) Zhao, D. Y.; Yang, P. D.; Huo, Q. S.; Chmelka, B. F.; Stucky, G. D. *Curr. Opin. Solid State Mater. Sci.* **1998**, *3*, 111.
(20) Bartl, M. H.; Boettcher, S. W.; Frindell, K. L.; Stucky, G. D. *Acc. Chem. Res.* **2005**, *38*, 263.
(21) Huo, Q. S.; Margolese, D. I.; Ciesla, U.; Feng, P. Y.; Gier, T. E.; Sieger, P.; Leon, R.; Petroff, P. M.; Schuth, F.; Stucky, G. D. *Nature* **1994**, *368*, 317.

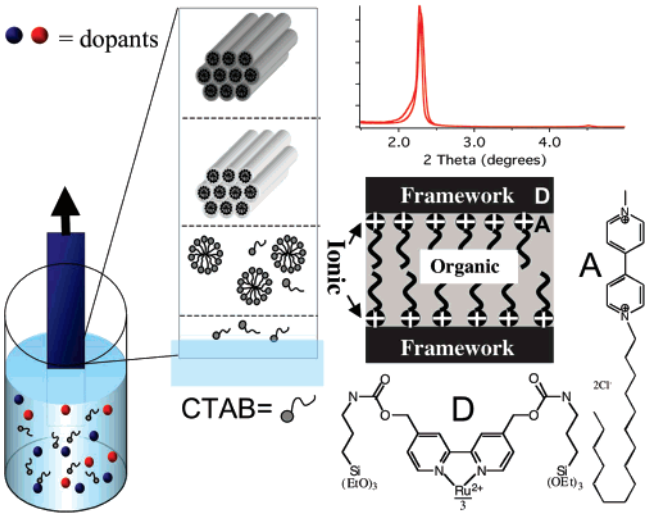

Figure 1. (Left) Withdrawing a silicon substrate from the sol leads to the formation of mesostructured silica thin films. The CTAB surfactant templates pores in 2D hexagonal arrays (Right bottom) The photoelectron donor (**D**) is located in the framework, while the electron acceptor (**A**) co-assembles with the surfactant. (Right top) XRD patterns for mesostructured films with and without **D** and **A**.

of its simplicity and reproducibility: everything needed is present in the starting sol, and 2D-hexagonal structured films with a uniform *d*-spacing are consistently produced.

In general, surfactant-templated sol−gel materials contain three spatially separated regions: the silica framework, the hydrophobic core of the templating liquid crystal phase, and the ionic interface region, which is the boundary between the first two regions. The unique physical and chemical properties of the regions in the mesostructured thin film allow these regions to be derivatized selectively. Three one-pot, one-step strategies have been developed for derivatizing silica thin films: the bonding, philicity, and bifunctional strategies. Using the bonding strategy, molecules are selectively placed in the silica framework by derivatizing them with condensable groups, thus making them part of the framework-forming material. The philicity strategy places molecules by taking advantage of their local solubility; hydrophobic molecules will be attracted to the micellar interior while ionic molecules will be attracted to the ionic interface. The bifunctional strategy uses a molecule with one hydrophobic end while the other end is an alkoxysilane that can attach to the framework. EISA has recently been used in our group to place photoactive molecules in the spatially separated regions of the mesostructure.[22−25]

In this paper we report the tunneling decay constant β for the silica region of mesostructured thin films. Deliberate placement techniques are used to simultaneously position a photoelectron donor in the silica framework and an electron acceptor into the ionic interface region. The photoelectron donor, **D**, and the electron acceptor, **A**, are shown in Scheme 1.

Because the donor and acceptor are confined in different regions, electron-transfer takes place through tunneling, and the

Scheme 1. Photoelectron Donor (**D**) and Electron Acceptor (**A**)

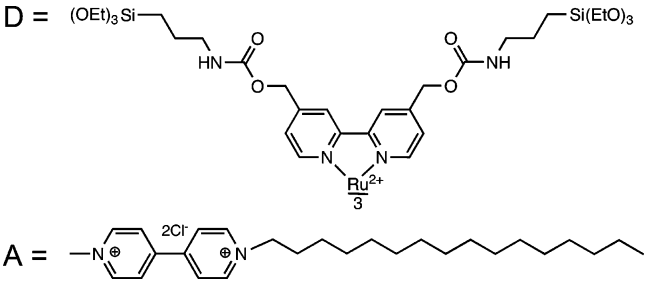

electron-transfer rate decreases exponentially with distance according to a model previously presented.[26] Numerical calculations are carried out in order to produce luminescence decay traces that fit the experimental data. Two variable parameters are used to fit the calculated traces to the experimental data. The first parameter is the quenching rate when the donor and acceptor are in contact, k_0. The second parameter is the tunneling decay constant, β. It is related to the decrease in electron-transfer rate as a function of distance and hence to the barrier presented to tunneling by the material. The calculated traces compare well to those obtained experimentally and allow insight into the tunneling barrier presented by silica manufactured by the process employed in this paper. β is an important parameter that is known for many systems. By combining deliberate placement techniques, spectroscopy, and calculations we report β for mesostructured silica and compare it to that for many other materials such as frozen glasses, alkane chains, and proteins (Figure 2).[27−30] Sol−gel thin films are of interest for electronic insulating applications. Our results show that mesostructured silica is an excellent insulator, better than frozen glasses and almost as good as vacuum.

Experimental Section

Preparation of *tris*-(4,4′-Methoxy-2,2′-bipyridine)−Ruthenium-(II) Dihexafluorophosphate. 4,4′-Methoxy-2,2′-bipyridine was prepared according to literature methods.[31,32] *tris*-(4,4′Methoxy-2,2′-bipyridine)−ruthenium(II) hexafluorophosphate was prepared by refluxing a slight excess of 4,4′-methoxy-2,2′-bipyridine and $RuCl_3$ in a methanol/ethanol mixture (2:8 v/v) for 72 h. The solvent was removed under reduced pressure, and the orange solid was dissolved in water. The final product was precipitated by addition of ammonium hexafluorophosphate and washed with ether. The NMR spectrum is the same as that reported.[33]

Preparation of *tris*-(4,4′-Silylated-2,2′-bipyridine)−Ruthenium-(II) Hexafluorophosphate: "D". The silylated donor (Figure 1) was prepared by refluxing isocyanatopropyl triethoxysilane (ICPES) and *tris*-(4,4′methoxy-2,2′-bipyridine)−ruthenium(II) dihexafluorophosphate in acetonitrile. Five milligrams of *tris*-(4,4′methoxy-2,2′-bipyridine)−ruthenium(II) dihexafluorophosphate was dried under vacuum at 100 °C overnight. The reaction vessel was allowed to cool to room temperature before 10 mL of acetonitrile, distilled from CaH_2, was added. After the *tris*-(4,4′methoxy-2,2′-bipyridine)−ruthenium(II) di-

(22) Hernandez, R.; Franville, A. C.; Minoofar, P.; Dunn, B.; Zink, J. I. *J. Am. Chem. Soc.* **2001**, *123*, 1248.
(23) Minoofar, P. N.; Hernandez, R.; Chia, S.; Dunn, B.; Zink, J. I.; Franville, A. C. *J. Am. Chem. Soc.* **2002**, *124*, 14388.
(24) Minoofar, P. N.; Dunn, B. S.; Zink, J. I. *J. Am. Chem. Soc.* **2005**, *127*, 2656.
(25) Nguyen, T. D.; Tseng, H. R.; Celestre, P. C.; Flood, A. H.; Liu, Y.; Stoddart, J. F.; Zink, J. I. *Proc. Natl. Acad. Sci. U.S.A.* **2005**, *102*, 10029.
(26) Blumen, A. *J. Chem. Phys.* **1980**, *72*, 2632.
(27) Miller, J. R.; Beitz, J. V. *J. Chem. Phys.* **1981**, *74*, 6746.
(28) Ponce, A.; Gray, H. B.; Winkler, J. R. *J. Am. Chem. Soc.* **2000**, *122*, 8187.
(29) Smalley, J. F.; Finklea, H. O.; Chidsey, C. E. D.; Linford, M. R.; Creager, S. E.; Ferraris, J. P.; Chalfant, K.; Zawodzinsk, T.; Feldberg, S. W.; Newton, M. D. *J. Am. Chem. Soc.* **2003**, *125*, 2004.
(30) Wenger, O. S.; Leigh, B. S.; Villahermosa, R. M.; Gray, H. B.; Winkler, J. R. *Science* **2005**, *307*, 99.
(31) Della Ciana, L.; Dressick, W. J.; Von Zelewsky, A. *J. Heterocycl. Chem.* **1990**, *27*, 163.
(32) Oki, A. R.; Morgan, R. J. *Synth. Commun.* **1995**, *25*, 4093.
(33) Collins, J. E.; Lamba, J. J. S.; Love, J. C.; McAlvin, J. E.; Ng, C.; Peters, B. P.; Wu, X. F.; Fraser, C. L. *Inorg. Chem.* **1999**, *38*, 2020.

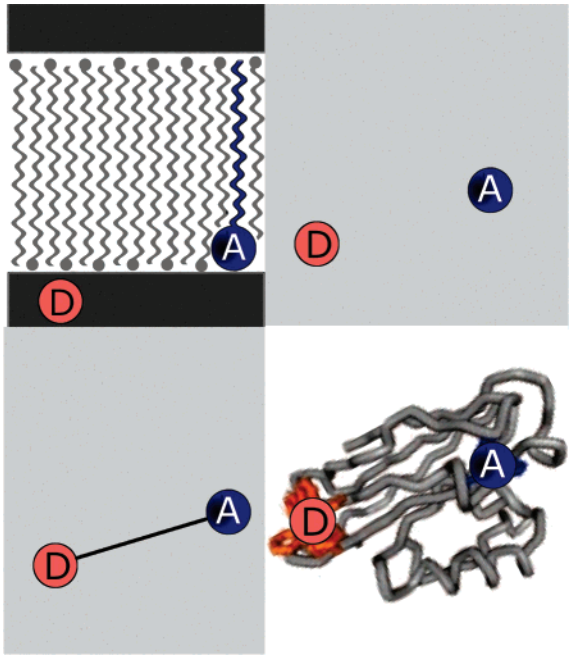

Figure 2. Time-resolved luminescence spectroscopy allows for comparison of electron tunneling barriers in systems as different as (top left) mesostructured sol−gel materials, (top right) rigid matrices, (bottom left) covalently linked donors and acceptors, and (bottom right) proteins.

hexafluorophosphate had dissolved, 30 μL of ICPES and 1 mL of triethylamine, dried over 4 Å molecular sieves, were added, and the solution refluxed for 24 h. The solvent was removed under reduced pressure and the product used directly without further purification. The NMR spectrum of the product proves the success of the coupling reaction by observing the shift of the two hydrogens next to the OH group on the bipyridines from 4.77 ppm (doublet) to 5.23 ppm (singlet) and the appearance of a peak at 5.91 ppm (triplet) attributed to the NH of the carbamide. The reaction was monitored using TLC where R_f (starting material) = 0.4 and R_f (product) = 0.85. The success of the coupling reaction can also be demonstrated using TLC (Merck Kieselgel 60, eluent H_2O/MeOH/MeCN/NaCl, 9.3:7.5:29.5:1) by adding a drop of 1 M HCl to the spot before starting the chromatography. The silane-coupled ruthenium complex does not move because its siloxane arms are now covalently linked to the TLC plate, while the R_f of the starting materials is the same as that without the addition of HCl.

Preparation of 1-Hexadecyl, 1′-methyl 4,4′-bipyridinium Dichloride. The electron acceptor, **A** (Figure 1), was prepared according to literature methods. The NMR spectrum of the synthesized compound is in agreement with that previously published.[34]

Sol Preparation and Film Synthesis. Films are synthesized as described previously.[13,23] First, a stock solution is prepared by mixing tetraethoxysilane (TEOS, the silicate precursor), ethanol, water, and HCl with mole ratios 1:3.8:1:(5×10^{-5}), respectively, and heating to 60 °C for 90 min. A 7.5-mL sample of this stock solution is then mixed with 1.032 mL of 0.07 M HCl and 0.344 mL of water, added by micropipetting, in a plastic beaker, and the resulting solution is stirred for 15 min and then aged for 15 min without stirring. At this point 20 mL of absolute ethanol is added to the mixture to make the sol. After the sol has been aged for 3 days, cetyl trimethyl ammonium bromide (CTAB), **A**, and **D** are added to achieve the desired concentrations where the **A** to **D** ratio ranges between 115:1 to 345:1. A strip of silicon, cleaned with piranha solution (H_2O_2/H_2SO_4, 1:4 by volume, heated to boiling for 1 h), is dipped into a Teflon reservoir containing the sol and withdrawn at a constant rate of 9.3 cm/min to yield the mesostructured film. The entire film-pulling apparatus is contained inside a controlled-humidity chamber, and all films are prepared at a relative humidity of 50 ± 5%.

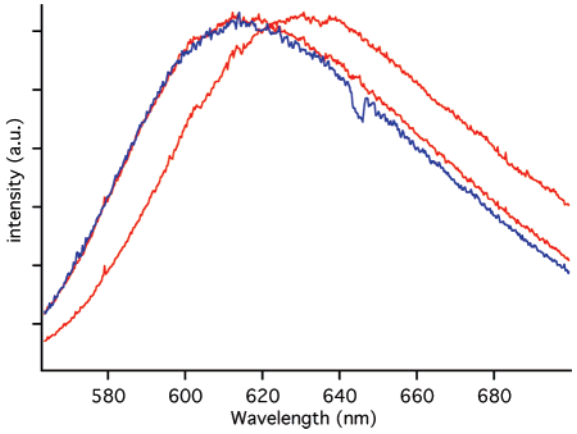

Figure 3. Luminescence spectra of Ru(II)−*tris*(bpy-ICPES) in the sol (far right) and in structured and nonstructured thin films (two leftmost traces).

Preparation of Films Containing A. While keeping the surfactant:Si ratio constant (both CTAB and **A** are surfactants) CTAB and **A** were added in the following ratios: 10:0, 9:1, 8:2, and 7:3. Films were prepared as described above in general sol preparation and film synthesis.

Instrumentation and Analysis. Time-resolved luminescence spectra and steady-state luminescence spectra were obtained using a Quantel Brilliant Nd:YAG laser to excite **D** (λ_{ex} = 355 nm, fwhm < 10 ns). The luminescence was passed through a 0.3 m monochromator with a 300 groove/mm grating. The light was dispersed onto a Roper Scientific PIMAX gated, intensified CCD. XRD spectra were obtained using a PANalytical X'Pert PRO.

Results

Mesostructure. All films contain **D** at a ratio of 1:1150 vs surfactant while the CTAB to quencher (**A**) ratio was 0:10, 1:9, 2:8, or 3:7. The first-order diffraction peak appears at 2θ = 2.3° ± 0.02° corresponding to a lattice spacing of 38.4 ± 0.3 Å. All films are crack free upon visual inspection, that is, the film surface is mirror-like, indicating the absence of defects detectable using visible light.

Luminescence Spectra. Incorporation of **D** is verified by steady-state emission spectroscopy. Luminescence (λ_{max} = 615 nm) is observed from the mesostructured film prepared from the sol containing **D**. The immediate environment around **D** changes markedly upon film formation, as is evident from the 15-nm blue shift of the luminescence spectrum when comparing the luminescence from the sol (λ_{max} = 630 nm) to the luminescence from the film (λ_{max} = 615 nm) (Figure 3). When CTAB is omitted but all other parameters left unchanged, luminescence from **D** in the unstructured film is also observed (λ_{max} = 614 nm). The small (1 nm) difference between the emission maxima in the unstructured and the structured films suggests that **D** is incorporated into the framework of the mesostructured film and not the surfactant core or the ionic interface. The incorporation of the **A** is proven by the decrease in luminescence lifetime of the luminescent electron donor **D** when the electron acceptor **A** is incorporated.

Time-Resolved Luminescence Spectroscopy. Batches of 12 films each were pulled, three at each of the four different concentrations of quencher. The films were aged in the humidity-controlled chamber overnight. Aging allows the condensation reaction to approach completion and lets solvent

(34) Hammarstrom, L.; Almgren, M.; Norrby, T. *J. Phys. Chem.* **1992**, *96*, 5017.

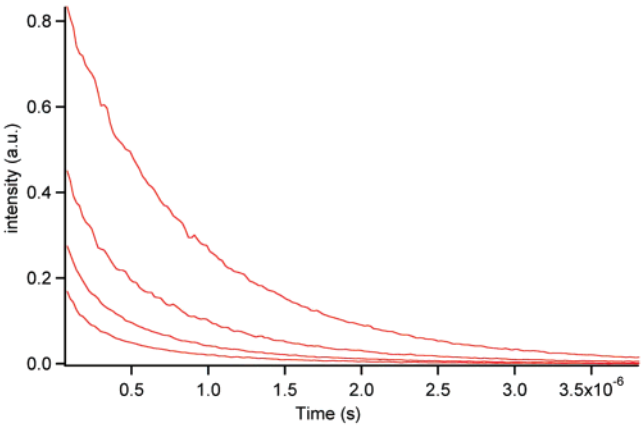

Figure 4. Luminescence decay ratios of **D** for CTAB to **A** of (top to bottom): 10:0, 9:1, 8:2, and 7:3. As the quencher concentration increases, the luminescence decay becomes increasingly non-exponential.

evaporate from the thin film. The next day luminescence measurements were made. Two hundred spectra, each of 10-ns integration time, were collected starting 200 ns before the 355-nm excitation pulse. Spectra were collected at 20-ns intervals until 3800 ns after the 255-nm pump. Since the films are only 100−200 nm thick, 200 accumulations were made for each time point in order to improve the signal-to-noise ratio. Spectra were collected for each of the three films at each concentration. The data was collected in the form of 2D matrices, which were used to construct the luminescence decay traces. The absolute intensity of the luminescence decay traces for all films with the same concentration of quencher was in good agreement, specifically, the run-to-run agreement was better than 3%. The three luminescence decay traces for each quencher concentration were combined into one luminescence decay trace. Baseline subtraction was achieved using an average of the intensity of the points collected before the 355-nm pump. The intensities of the four traces were normalized versus the no-quencher luminescence decay trace. The normalized traces were used to fit calculated luminescence decay traces.

Examples of luminescence decay traces for films containing **D** only, and **D** and **A** at the aforementioned ratios, are shown in Figure 4. When doing repeated accumulations, there is always the possibility of decomposition of the donor or acceptor over time. In order to verify that the donors and acceptors are not degrading over the time scale of the experiment, the luminescence intensity was checked at the beginning of the experiment as well as at the end. The luminescence intensity stayed the same, proving that the donor was not decomposing. The acceptor was proven not to decompose by obtaining multiple luminescence decay traces of the same film. Lifetimes stayed the same for those measurements, proving that the degree of quenching and hence the quencher concentration remained constant.

THEORETICAL MODEL

The model used to analyze the data is an expansion of a model presented earlier.[26] It is assumed that the noncontact electron transfer between the donor and acceptor separated by a distance R takes place through tunneling, and that the probability of electron transfer decreases exponentially with R.[26] Electron transfer takes place from the excited-state of the photoelectron donor. The excited-state of the photoelectron donor can be deactivated by a number of processes including relaxation through emission of a photon, nonradiative relaxation, and electron transfer to an electron acceptor. The luminescence intensity decay trace, $I(t)$, of an electron donor in the presence of quenchers can be written as:

$$I(t) = I_0(t) \prod_i \exp(-t \times k_0 \times \exp(-\beta(R_i - R_0))) \quad (1)$$

where $I_0(t)$ is the intensity as a function of time in the absence of quenchers, k_0 is the contact quenching rate, β is the decay constant of the contact quenching rate, R_0 is the center to center distance for the donor and acceptor, and i indicates the ith acceptor and R_i is the distance between the donor and acceptor i.

Both electron donors and acceptors are confined to their respective regions of the mesostructured thin film but are distributed in a random fashion in these regions. The electron acceptors are restricted to the inner surface of the pores, which are packed in a 2D-hexagonal pattern. The electron donors are located in the space between the tubes, but not inside the tubes or in the ionic interface. For randomly distributed donors and acceptors there is a closed formula solution to eq 1.[26]

In the case of the mesostructured material the problem was solved numerically. Simulations are set up where distances between a donor and many acceptors are found, given the constraints stated above. The distances are used to calculate a luminescence decay spectrum. This process is repeated 4000 times to get an average representative of actual experimental conditions. $I_0(t)$ is experimentally determined from the luminescence decay in the absence of quenchers. The calculated decay traces are compared to those experimentally obtained. The "goodness" of the fit is determined by calculating S (eq 2) for a certain pair of β and k_0. S is the least-squares value, y_i is the experimental value at time point i, f is equal to $I(t)$ in eq 1, and R is an array of donor−acceptor distances.

$$S = \sum_{i=1}^{n} (y_i - f(k_0,\beta,R))^2 \quad (2)$$

The β and k_0 values together with S are recorded. This method yields a best fit that is unique, i.e., there is a β and k_0 pair that yields a unique minimum S.

Discussion

Mesostructure and Donor/Acceptor Placement. The films studied were made through evaporation induced self-assembly (EISA).[13] A homogeneous solution is prepared containing TEOS, CTAB, HCl, and water. To this solution is added **D** and **A** to desired concentrations. A silicon substrate is dipped into the solution after which the substrate is retracted, pulling with it a thin film of liquid. Ethanol will evaporate preferentially from the film of liquid, raising the concentrations of water, acid, and surfactant. This change increases the rate of condensation of the silica monomers and forces the surfactant to form the desired liquid crystal structure. The silica oligomers arrange themselves around the liquid crystal phase, and condensation continues, yielding the surfactant-templated, nanostructured silica thin film as illustrated for CTAB in Figure 1. The final film is 100−200 nm thick. The XRD patterns obtained for the mesostructured films are consistent with 2D-hexagonal mesostructure with the main diffraction peak positioned at $2\theta = 2.3° \pm 0.02°$ corresponding to a lattice spacing of 38.4 ± 0.3 Å.

Surfactant-templated mesosotructured silica thin films have three regions with distinct and differing physical properties. These regions arise from the two main components of the sol and the interface formed between them. The three regions are the following: the silica framework, the hydrophobic micelle core, and the ionic interface between the surfactant and the silica. Because of the differences in physical and chemical properties of the three regions, strategies exist to place molecules deliberately in any of the regions.

The approaches for selective placement of **D** and **A** used in this paper are the bonding strategy and the philicity strategy.[22,23] In the "philicity" strategy, placement of molecules is achieved by taking advantage of the local solubility of different molecules. For example, hydrophobic molecules will go into the hydrophobic region, while ionic molecules will go into the ionic region. Using the bonding strategy, molecules are placed in the framework by making them a building block of the framework. The molecule of interest is derivatized such that it itself undergoes hydrolysis and condensation. The photoelectron donor (**A**) was placed in the silica framework by derivatizing ruthenium(II)−*tris*-(4,4′-methoxy-2,2′-bipyridine) with co-condensable alkoxysilane arms, thus making it a part of the framework. The successful incorporation of the ruthenium moiety into the silica region is supported by the almost identical emission spectra observed in mesostructured (λ_{max} = 615 nm) and amorphous (λ_{max} = 614 nm) films (Figure 3), which are substantially different from the solution spectrum (λ_{max} = 630 nm). The electron acceptor was placed selectively in the ionic interface by utilizing the philicity strategy and a methyl viologen analogue with surfactant properties, 1-hexadecyl,1′-methyl 4,4′-bipyridine dichloride (**A**).[34] **A** is known to form micelles by itself[35] as well as to fully incorporate into CTACl micelles while retaining its ability to function as a reversible electron acceptor.[36,37] The electro-active part of the molecule is the headgroup, and it is anchored in place by its association with the micellar core via its hexadecyl tail.

The purpose of spatial separation of **D** and **A** is to measure the tunneling decay constant β for the silica region of mesostructured thin films. A donor/acceptor pair with well-known and exhaustively studied electron-transfer properties was chosen. Ruthenium(II)−*tris*(bipyridine) is a well-known photoelectron donor, and methyl viologen is an extensively used electron acceptor.[38] The problem with these two prototypical candidates is that there is little control over how and where they incorporate into the thin film. It is likely that both underivatized Ru(II)−*tris*(bipyridine) and methyl viologen will distribute themselves throughout the ionic interface and silica framework and electron-transfer would take place by contact electron transfer in the silica framework and/or contact electron transfer in the ionic interface in addition to electron transfer by tunneling from the donor to acceptor, both along the ionic interface and through the silica region. Separating the contributions from the different rections would be difficult. Experimental quenching data show that the electron donor and acceptor are indeed separated and that the degree of quenching is much less than that for the corresponding concentrations of ruthenium−*tris*(bipyridine) and methyl viologen in solution. The incorporation of **D** and **A** have no effect on the mesostructure as confirmed by XRD measurements. Care must be taken because incorporation of some dopants can drastically affect the mesostructure formed.[39]

Calculation of the Coefficient β. When electron-transfer takes place through tunneling, the probability of tunneling decreases exponentially with the donor−acceptor distance where the exponential decay constant is referred to as β (eq 1). β varies greatly depending on the nature of the media through which the electron has to tunnel. The greatest barrier to tunneling and hence the largest β is that for vacuum ($\beta = 2.9-4.0$ Å^{-1}), while small values have been measured for systems such as conjugated organic polymers.[30] It should be pointed out that β is predicted to depend on the energy difference between the tunneling electron and the reduced and oxidized states of the intervening material.[30] Experimental data, however, suggest that β is primarily a function of the bridge and relatively independent of the donor and acceptor.[30,40] Blumen[26] has outlined how to theoretically predict the degree of electron transfer between a donor and acceptors in the case of electron transfer through tunneling. In the case when electron transfer can be observed due to the change in luminescence lifetime of the donor, the luminescence decay trace can be described by eq 1. For certain donor−acceptor geometries an analytical solution that describes the luminescence decay has been derived.[26] This analytical solution has been used to fit calculated spectra to experimental results in order to extract β and k_0 values for frozen glasses, proteins, and conjugated bridges.[30]

For 2D-hexagonal geometry an analytical solution does not exist, and the luminescence decay trace has to be calculated numerically. The aim of the calculations is to determine which β and k_0 pair is best able to fit the experimentally obtained luminescence decay trace, keeping in mind that the **D** and **A** are confined to specific regions. In order to achieve this, a brute force approach is taken. For each pair of β and k_0, an ensemble average luminescence decay trace is calculated and compared to that experimentally obtained, where the goodness of the fit is measured by S (eq 2). A contour plot is created where the x- and y-axes are β and k_0, respectively, and the z-axis is S. The minimum value of S gives the β and k_0 pair that best fits the experimentally obtained data.

The calculations are carried out as follows using an iterative procedure. Step one is to determine the positions of the surfactant headgroups in the mesostructured silica thin film using the known 3D structure of the material and the d-spacing. A list of the positions of the headgroups in space is constructed. The second step is to choose which of the headgroups are the active paraquat **A** headgroups. The **A** headgroups are chosen randomly from the list of possible positions using a random number generator. The constraint that the ratio of **A** to CTAB headgroups matches the ratio used experimentally is imposed. The third step is to position **D**. Because the donor is located in the silica framework, a position for **D** is chosen randomly under the constraint that it be neither in the ionic interface nor in the hydrophobic region. The fourth step is to calculate the straight line distance from **D** to all **A**. The list of distances obtained is

(35) Krieg, M.; Pileni, M. P.; Braun, A. M.; Gratzel, M. *J. Colloid Interface Sci.* **1981**, *83*, 209.
(36) Lee, C. W.; Oh, M. K.; Jang, J. M. *Langmuir* **1993**, *9*, 1934.
(37) Brugger, P. A.; Infelta, P. P.; Braun, A. M.; Gratzel, M. *J. Am. Chem. Soc.* **1981**, *103*, 320.
(38) Bock, C. R.; Meyer, T. J.; Whitten, D. G. *J. Am. Chem. Soc.* **1974**, *96*, 4710.
(39) Garcia, J. A.; Valverde, G.; Zink, J. I. *Langmuir* **2003**, *19*, 4411.
(40) Lewis, F. D.; Liu, J. Q.; Weigel, W.; Rettig, W.; Kurnikov, I. V.; Beratan, D. N. *Proc. Natl. Acad. Sci. U.S.A.* **2002**, *99*, 12536.

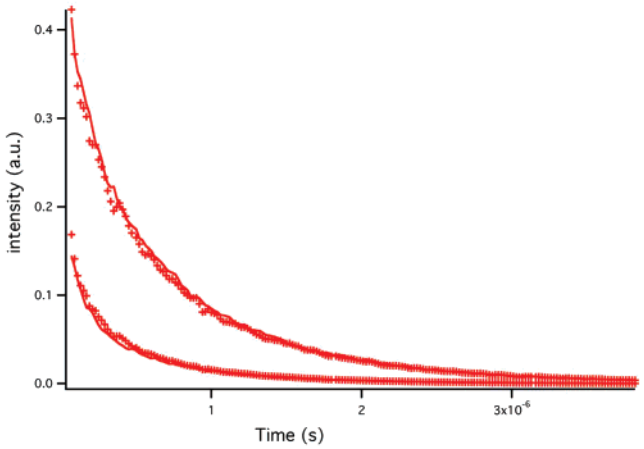

Figure 5. Calculated fits to experimental luminescence decays. β and k_0 are optimized in order to obtain the best fit.

sorted in ascending order, and the seven shortest distances are used in the calculation. The fifth step is to use the list of distances, together with the initial trial values of β and k_0, to calculate a luminescence decay trace using eq 1. This calculated luminescence decay trace is for one specific donor−acceptor configuration only and will therefore not resemble the experimentally obtained luminescence decay trace. The calculated trace is saved in a temporary vector. In order to calculate a trace that is comparable to that experimentally obtained, it must be an ensemble average. To construct this ensemble average steps one through five are repeated for a total of 4000 times, after which the sum of the traces is divided by 4000. The goodness of the fit to the experimental data is calculated using eq 2. The "goodness" of the fit together with the β and k_0 used to calculate it provide one point in the contour plot. The procedure is repeated using physically relevant combinations of β and k_0, and the minimum S in the contour plot is found.

Calculations fitted to three different quencher concentrations yielded a contact quenching rate $k_0 = 1 \times 10^{(13.5\pm0.8)}$ s^{-1} and $\beta = 2.5 \pm 0.4$ Å^{-1}. Examples of experimental data and calculated fits for quencher concentrations 1:9 and 3:7 are shown in Figure 5.

In order to determine whether the obtained k_0 is reasonable, it is compared to the electron-transfer rate between a covalently linked ruthenium−*tris*-(bipyridine) and methyl viologen moiety. A previous study measured the electron-transfer rate between the ruthenium−*tris*-(bipyridine) and methyl viologen moiety linked by a CH_2 group.[41] The obtained electron-transfer rate (2.5×10^{11} s^{-1}) is lower than k_0 as measured by us, which is expected since the donor and acceptor are not in direct contact but are held apart by a CH_2 group. β is positive, and smaller than that for vacuum, which is the upper limit.[30] It is therefore a reasonable value. Since, as mentioned earlier, β appears to be primarily dependent on the bridge properties, it can be compared to values for many other systems measured using different donor−acceptor pairs.

In addition to supporting the successful separation of electron donors and acceptors in mesostructured silica the calculations yield measurements of the important physical parameters, k_0 and β. The distance decay constant β has been calculated for a number of glasses.[30] Going from high to low β, examples of known values are for vacuum (2.9−4 Å^{-1}), methyl tetrahydrofuran glass (1.57−1.67 Å^{-1}), aqueous glass (1.55 − 1.65 Å^{-1}), and toluene glass (1.18 − 1.28 Å^{-1}). Furthermore, data have been compiled on β values for donor−bridge−acceptor systems that exhibit exponential distance dependences of the electron-tunneling probability.[30] For xylyl bridges $\beta = 0.76$ Å^{-1}, for alkane bridges $\beta = 1.0$ Å^{-1}, and for β-strand bridges in ruthenium-modified azurin, $\beta = 1.1$ Å^{-1}. An STM study of electron tunneling through silica showed that, using a sample bias lower than ±2 V, the tunneling current was under the detection limit which indicated that the oxide film was insulating.[42] It is clear from the data presented that the tunneling barrier in mesostructured glass is quite high compared to those measured for many other systems (Figure 6).

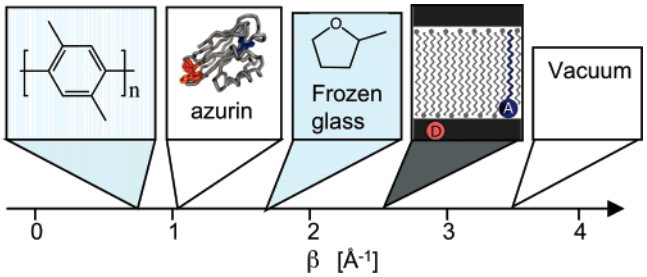

Figure 6. Comparison of the β value for mesostructured silica with those of xylene bridges, azurin, frozen MTHF glass, and vacuum. The silica framework is an excellent insulator.

The silica framework is highly microporous; the silica walls are not composed of a dense SiO_2 matrix but rather a spongelike SiO_2 matrix with micropores. This structure would give the tunneling electron two options. First it could tunnel through regions that are primarily gas-filled micropores. Second, it could follow Si−O−Si bonds, in which case the tunneling distance is longer than the distance measured as a straight line. Both options would yield a higher observed β. The silica framework in mesostructured silica materials is an efficient insulator.

Summary

Silicate thin films with highly ordered nanostructure containing spatially separated electron donor and acceptor molecules are synthesized. The films consist of a silicate framework that holds in place a 2D-hexagonal structure templated by an ionic surfactant. Pairs of molecules consisting of a photoelectron donor ruthenium complex and an electron acceptor methyl viologen derivative are placed in the framework and the ionic interface, respectively, using a one-step, one pot synthesis. The ruthenium complex contains ethoxysilane groups that bond to and form part of the framework, and the placement is an example of the "bonding" strategy. The methyl viologen derivative is localized in the ionic interface region of the surfactant, and its placement is an example of the "philicity" strategy.

Spectroscopic data show that the photoelectron donor is incorporated into the framework. Electron transfer is verified by observing the decrease in luminescence lifetime as the electron acceptor concentration is increased. The tunneling decay constant β of the silica region of the mesostructured thin films is calculated from luminescence lifetime data. Numerical fits

(41) Lomoth, R.; Haupl, T.; Johansson, O.; Hammarstrom, L. *Chem. Eur. J.* **2002**, *8*, 102.

(42) Watanabe, H.; Baba, T.; Ichikawa, M. *J. Appl. Phys.* **2000**, *87*, 44.

to the luminescence decay traces give information about the contact quenching rate, k_0, as well as the tunneling decay constant, β. The β value calculated for mesostructured silica is found to be quite high, which is consistent with the microporous nature of silica produced this way as well as the large band gap of silica glass. Combining the ability to place molecules precisely within the mesostructure coupled with numerical calculations has yielded information that would be hard to obtain by other methods and allows us to compare the tunneling decay constant β for mesoporous silica thin films to many other systems.

Acknowledgment. This work was supported by NSF Grants CHE 0507929 and DMR 0103952. E.J. thanks Dr. Edward Plummer for helpful discussions.

JA075323A